energies

MDPI

Article

On the Influence of Solar Radiation on Heat Delivered to Buildings for Heating

Tomasz Cholewa [1,*], Agnieszka Malec [1], Alicja Siuta-Olcha [1], Andrzej Smolarz [2], Piotr Muryjas [2], Piotr Wolszczak [3], Łukasz Guz [1], Marzenna R. Dudzińska [1] and Krystian Łygas [3]

[1] Faculty of Environmental Engineering, Lublin University of Technology, Nadbystrzycka 40B, 20-618 Lublin, Poland; a.malec@pollub.pl (A.M.); a.siuta-olcha@pollub.pl (A.S.-O.); l.guz@pollub.pl (Ł.G.); m.dudzinska@pollub.pl (M.R.D.)
[2] Faculty of Electrical Engineering and Computer Science, Lublin University of Technology, Nadbystrzycka 38A, 20-618 Lublin, Poland; a.smolarz@pollub.pl (A.S.); p.muryjas@pollub.pl (P.M.)
[3] Faculty of Mechanical Engineering, Lublin University of Technology, Nadbystrzycka 36, 20-618 Lublin, Poland; p.wolszczak@pollub.pl (P.W.); krystian.lygas@gmail.com (K.Ł.)
* Correspondence: t.cholewa@pollub.pl; Tel.: +48-81-538-44-24

Abstract: Nowadays, the attention of designers and service providers is especially focused on energy efficiency and integration of renewable energy sources (RES). However, the knowledge on smart devices and automated, easily applicable algorithms for optimizing heating consumption by effectively taking advantage of solar heat gains, while avoiding overheating, is limited. This paper presents a simple method for taking into account the influence of solar heat gains in the form of solar radiation for the purposes of forecasting or controlling thermal power for heating of buildings. On the basis of field research carried out for seven buildings (five residential buildings and two public buildings) during one heating season, it was noticed that it was justified to properly narrow down the input data range included in the building energy model calculations in order to obtain a higher accuracy of calculations. In order to minimize the impact of other external factors (in particular wind speed) affecting the heat consumption for heating purposes, it was recommended to consider the data range only at wind speeds below 3 m/s. On the other hand, in order to minimize the impact of internal factors (in particular the impact of users), it was suggested to further narrow down the scope of the input data to an hour (e.g., 10–14 in multi-family residential buildings). During these hours, the impact on users was minimized as most of them were outside the building.

Keywords: integration of RES; solar heat gains; solar radiation; building energy model; prediction methods

Citation: Cholewa, T.; Malec, A.; Siuta-Olcha, A.; Smolarz, A.; Muryjas, P.; Wolszczak, P.; Guz, Ł.; Dudzińska, M.R.; Łygas, K. On the Influence of Solar Radiation on Heat Delivered to Buildings for Heating. *Energies* **2021**, *14*, 851. https://doi.org/10.3390/en14040851

Academic Editor: Jae-Weon Jeong
Received: 30 November 2020
Accepted: 2 February 2021
Published: 6 February 2021

1. Introduction

Regarding climate change and emission of greenhouse gases, the use of renewable energy sources (RES), such as solar radiation, in buildings is very common nowadays [1,2]. Solar radiation may be used in buildings in the form of active systems, such as flat solar collectors [3], but is recommended especially if used passively without special additional investment and exploitation cost.

This may be, for example, passive heating through glazing [4], which may reduce the heat used for heating in the winter season [5].

However, due to solar heat gains, the overheating may occur in buildings not only during heat waves [6] or normal exploitation during the summer period [7,8], but also during the winter season [9].

This may be due to inaccurate control methods of heat supply to a room or building, which does not fully or properly take into account the presence and influence of solar gains on energy consumption, which was shown in the example of co-heating tests [10].

In this light, Danov et al. [11] proposed the method for introducing the solar gain into the calculation of total heat loss coefficient. Knudsen and Petersen [12] underlined that

it is not easy to simultaneously minimize overheating and energy costs; therefore, they proposed economic model predictive control for space heating. The use of model predictive control (MPC) may significantly reduce the energy consumption for heating [13], but there are still some barriers in wide application of such control methods [14], connected also with influence of external and internal factors on the building energy consumption [15]. That is why a lot of studies try to address these issues [16–19].

However, to the best of the authors' knowledge, the amount of information about smart devices and automated, easily applicable algorithms to optimize heating consumption by effectively taking advantage of solar heat gains, while avoiding overheating, is limited.

This work contributes to this field and presents recommended parameters as well as a simple, widely applicable methodology for proper consideration of solar radiation in building energy model.

Section 2 presents the buildings and methodology of research. Section 3 describes the results and discussion regarding the methodological aspects of considering solar radiation in the creation of a building energy model.

2. Materials and Methods

The field tests were carried out in 7 buildings (Table 1) located approximately 500 m from each other in the Lubelskie Voivodeship in Poland. These included two public buildings (a court building and a store building) and five multi-family residential buildings. The selection of such a set of buildings for this research was aimed at showing the obtained dependencies of the solar radiation influence on heat consumption not only in residential buildings, but also public buildings.

Table 1. Characteristic of the analyzed buildings.

Building	Building Type	Heated Floor Area (m^2)
B1	multifamily	4195
B2	multifamily	3970
B3	multifamily	2910
B4	multifamily	1845
B5	multifamily	4264
B6	public–courthouse	9248
B7	public–shop	280

The buildings had thermal insulation in the external walls and the roof. However, the methodology of determining the influence of solar radiation on the amount of thermal power supplied to a building for heating is a universal one, and that is why it may be successfully applied to the buildings without thermal insulation. Besides, because of the simplicity of this method, it is not required to know the emissivity of the building or its parts, solar absorptivity, or surface temperatures of parts of the building (windows, walls, and roof), which necessitates conducting additional measurements and very detailed calculations, and in this way may limit wide usage of this approach.

Each building was equipped with a central hydronic heating system with vertical risers connected to convection radiators. The analyzed buildings were supplied with heat from the district heating network through a thermal node located on the ground floor of each building, which participated in the heat exchange between the heating system and the heating and domestic hot water installation in analyzed buildings.

In each of the heating nodes, a calibrated heat meter was used to measure the heat power supplied to a given building for heating purposes (Qh). The research consisted of the continuous measurement of the heat power supplied to the analyzed buildings for heating (Qh) in the period from 1 October 2015 to 30 April 2016.

In addition to the parameters related to the heat supply to the analyzed buildings, the following weather parameters were also measured using a weather station located

in the immediate vicinity of the analyzed buildings: outdoor temperature, wind speed (average and maximum), solar insolation (*S_insol* in J/cm^2), cloudiness (*Cloud_1* in %), and cloudiness (*Cloud_2* in octants).

Due to the large amount of measurement data, this analysis used only the data related to 1 h.

3. Results

This section presents an analysis of the obtained research results, which was divided into two stages. Section 3.1 shows the analysis of the influence of solar radiation on the heat power supplied to the buildings for heating, in order to properly narrow down the scope of input data for further analysis. Then, Section 3.2 presents the results of the outdoor temperature correction with regard to the parameters characterizing solar radiation.

3.1. Solar Radiation and Heat Power Supplied for Heating

Solar radiation acting on the building envelope has an impact on the temporary demand for heat power during the entire heating season. In turn, the intensity of solar radiation may be influenced by clouding of the atmosphere caused by natural phenomena, such as cloudiness or dust pollution. The influence of this external factor on the amount of heat power supplied to buildings can be taken into account, involving solar insolation or cloudiness. These parameters are available in the databases of weather applications and services, both in the field of historical and forecast data.

However, it should be remembered that, in parallel with solar radiation, many other external factors (in particular, outdoor air temperature and wind speed) and internal factors (user behavior and preferences), which require an appropriate computational approach, also affect the building.

Therefore, in the first place, a detailed analysis related to the impact of external factors related to solar radiation (*S_insol*, *Cloud_1*, and *Cloud_2*) on the heat power supplied to the building for heating purposes was carried out at different hourly ranges of data included in the analysis and wind speed values (please see Table 2), for the purpose of appropriately narrowing down the data scope for further analysis in Section 3.2.

Table 2. Analyzed conditions of external factors related to solar radiation.

External Factor	Ranges of External Factor	Ranges of Wind Speed	Hourly Ranges
solar insolation (*S_insol*) (J/cm^2)	0–35; 35–100; 100–200; > 200;	v < 3 m/s; 3 ≤ v < 6 m/s; V > 6 m/s;	6 am–6 pm; 10 am–2 pm;
cloudiness (*Cloud_1*) (%)	0–20; 20–40; 40–60; 60–80; 80–100;	v < 3 m/s; 3 ≤ v < 6 m/s; V > 6 m/s;	6 am–6 pm; 10 am–2 pm;
cloudiness (*Cloud_2*) (octants)	0–2; 3–5; 6–7; 8;	v < 3 m/s; 3 ≤ v < 6 m/s; V > 6 m/s;	6 am–6 pm; 10 am–2 pm;

Therefore, in the case of solar insolation (*S_insol*), the dependencies of the heat power supplied to the analyzed buildings in relation to the outdoor temperature were determined for *S_insol* from the ranges: at wind speeds (average and maximum) from three different ranges (v < 3 m/s, 3 ≤ v <6 m/s, and for v > 6 m/s) and two hourly intervals, from 6 am to 6 pm and from 10 am to 2 pm.

In the case of cloudiness expressed in % (*Cloud_1*) and cloudiness expressed in octants (*Cloud_2*), the dependencies of heat power supplied to the analyzed buildings in relation

to the outdoor temperature at wind speeds (average and maximum) from three different ranges ($v < 3$ m/s, $3 \leq v < 6$ m/s and for $v > 6$ m/s) and two hourly intervals from 6 am to 6 pm and from 10 am to 2 pm for *Cloud_1* from the ranges 0–20%, 20–40%, 40–60%, 60–80%, and 80–100%; and for *Cloud_2* in the ranges 0–2 octant (little cloudiness), 3–5 octants (moderate cloudiness), 6–7 (cloudy), and 8 (overcast), were determined.

The results of the analyses for individual cases were developed in the form of graphs and were used to determine the correlation equations together with the determination coefficients (R^2), which were presented in the Figures 1–3 for building B2 and B5 and in the form of an exemplary summary of the obtained determination coefficients for building B5 (Table 3).

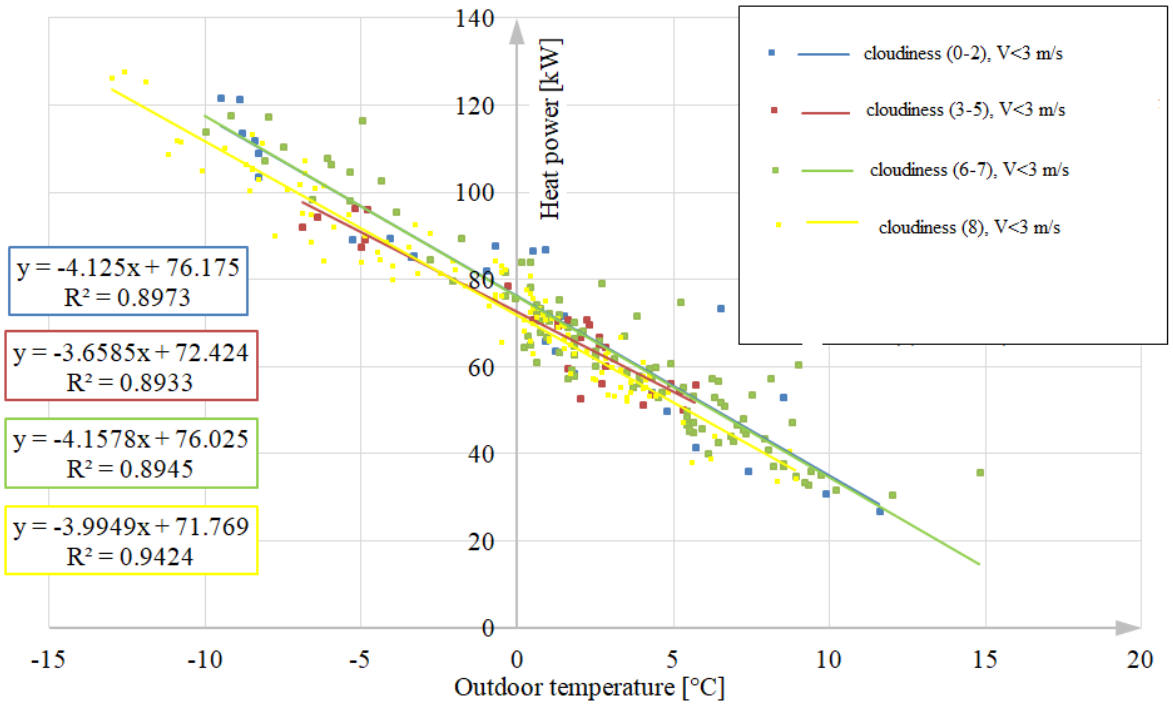

Figure 1. Dependence of heat power (kW) on the outdoor temperature (°C) and cloudiness (octants), for maximum wind speed below 3 m/s, 6 am–6 pm, and multi-family building B2.

On the basis of Figures 1 and 2, it can be seen that the logical dependencies of the parameters related to the influence of solar radiation on the heat power supplied to buildings are not always obtained, because with increasing cloudiness, the demand for heat power should clearly increase. The reason for this may be the influence of other external factors or users on the heat power needed for heating, as well as the different reactions of individual buildings to a given external factor.

On the other hand, in the case of solar insolation (Figure 3), the logical dependencies of heat power (*Qh*) on *S_insol* were obtained for building B5, and the same data range (for the average wind speed below 3 m/s, for 10 am–2 pm) as in the case of *Cloud_1*. This is because the demand for heat power decreases with increasing solar insolation.

Therefore, apart from the logical analysis of the obtained equations, it is also justified to carry out a detailed analysis of the obtained values of the determination coefficients (example for building B5 in Table 3), which show how accurately the given equation fits the obtained results.

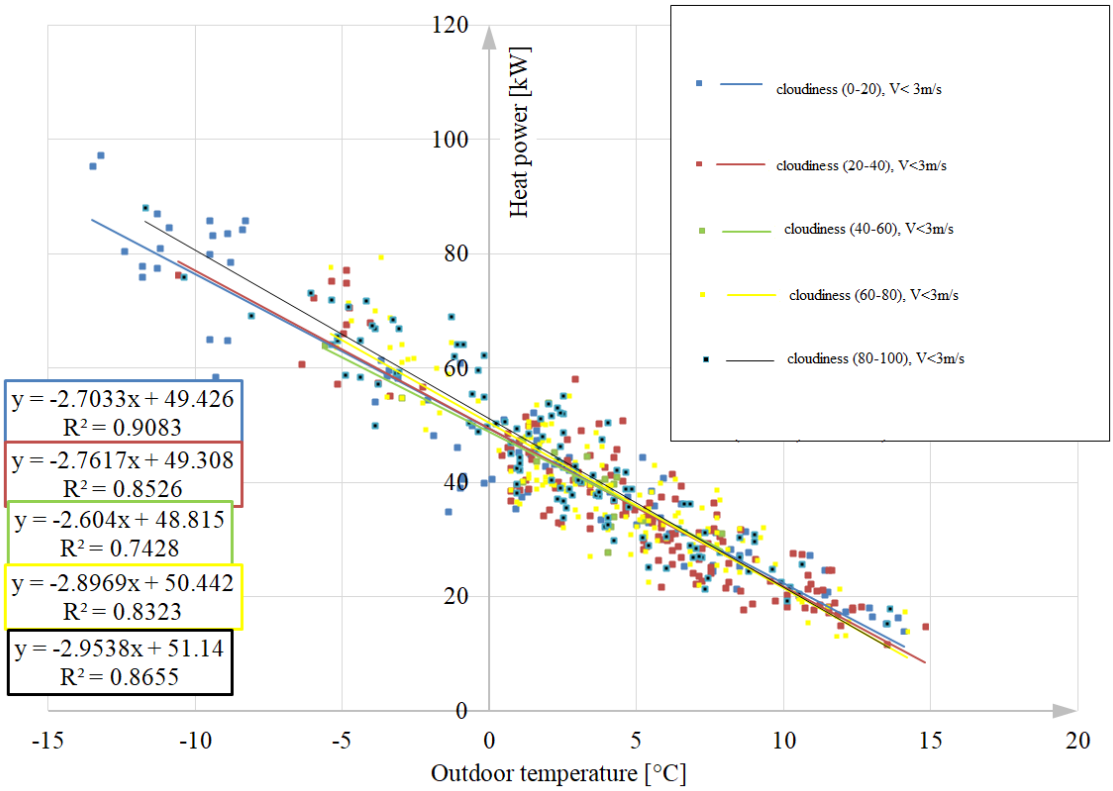

Figure 2. Dependence of heat power (kW) on the outdoor temperature (°C) and cloudiness (%), for average wind speed below 3 m/s, 10 am–2 pm, and multi-family building B5.

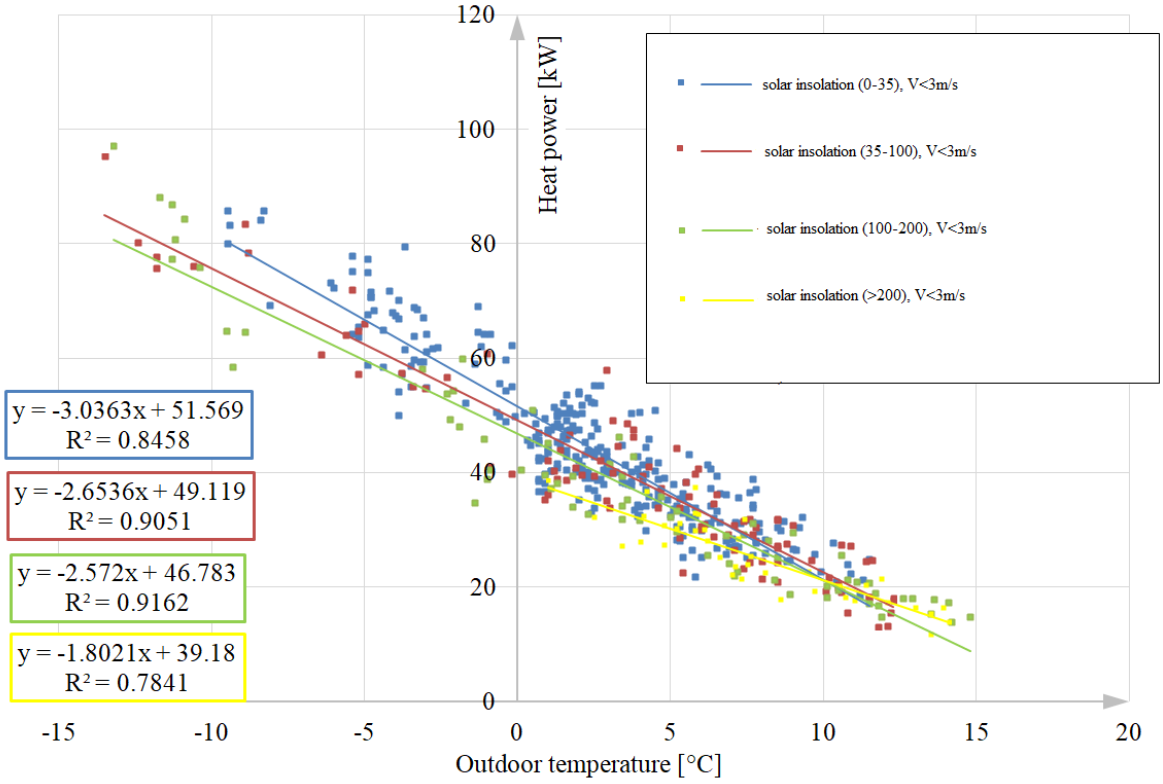

Figure 3. Dependence of heat power (kW) on the outdoor temperature (°C) and solar insolation (J/cm^2), for average wind speed below 3 m/s, 10 am–2 pm, and multi-family building B5.

Table 3. Summary of the determination coefficients (R^2) of the equations developed for multi-family building B5 for 6 am–6 pm and for 10 am–2 pm in parentheses.

Parameter	Wind Speed	v < 3 m/s	3–6 m/s	v ≥ 6 m/s
0–2 octants	average	0.9013 (0.9083)	0.8431 (0.7886)	- (-)
	maximum	0.9548 (0.9741)	0.9125 (0.9186)	0.8593 (0.8782)
3–5 octants	average	0.8212 (0.8466)	0.7675 (0.8303)	1 (1)
	maximum	0.8363 (0.8131)	0.7960 (0.8082)	0.8026 (0.8579)
6–7 octants	average	0.8307 (0.8600)	0.8011 (0.8201)	0.9911 (1)
	maximum	0.8238 (0.8628)	0.8329 (0.8538)	0.8062 (0.8304)
8 octants	average	0.8585 (1.000)	0.8342 (-)	0.9647 (-)
	maximum	0.8496 (-)	0.855 (-)	0.8866 (-)
0–20%	average	0.9094 (0.9083)	0.7674 (0.7886)	- (-)
	maximum	0.951 (0.9741)	0.9192 (0.9186)	0.8796 (0.9022)
20–40%	average	0.8055 (0.8526)	0.8116 (0.8526)	- (-)
	maximum	0.8612 (0.9118)	0.7787 (0.8008)	0.8039 (0.8648)
40–60%	average	0.8673 (0.7428)	0.5918 (0.6515)	1 (1)
	maximum	0.9016 (-)	0.9306 (0.8934)	0.5852 (0.8069)
60–80%	average	0.7985 (0.8323)	0.7565 (0.7698)	0.9911 (1)
	maximum	0.7337 (0.8737)	0.8218 (0.8360)	0.7438 (0.7687)
80–100%	average	0.8501 (0.8655)	0.8124 (0.8661)	0.964 (-)
	maximum	0.858 (0.8772)	- (-)	0.8529 (0.8821)
0–35 J/cm^2	average	0.8450 (0.8458)	0.8034 (0.8324)	0.9385 (1.0000)
	maximum	0.8562 (0.8847)	0.8331 (0.8254)	0.8339 (0.8514)
35–100 J/cm^2	average	0.9051 (0.9051)	0.7859 (0.8355)	0.9858 (1.0000)
	maximum	0.9329 (0.8662)	0.8964 (0.8920)	0.8522 (0.8673)
100–200 J/cm^2	average	0.9085 (0.9162)	0.7832 (0.7975)	- (-)
	maximum	0.9750 (0.9718)	0.8879 (0.9068)	0.8831 (0.8806)
>200 J/cm^2	average	0.8172 (0.7841)	0.8086 (0.6992)	- (-)
	maximum	- (-)	0.9061 (0.8759)	0.7424 (0.7472)

In order to decide which of the wind speed ranges ($v < 3$ m/s, $3 \leq v < 6$ m/s, $v > 6$ m/s) is the most reliable and shows the smallest disturbances (has the highest coefficient of determination), the arithmetic averages of coefficients of determination were calculated. The average values were calculated for each of the wind speed ranges, separately for each building. Then, the arithmetic mean of all individual mean values of the determination coefficients of the analyzed buildings were calculated, separately for residential and public buildings, as shown in Figure 4. This analysis does not take into account the division into average and maximum wind speed.

Figure 4 shows that the highest coefficients of determination occur for the wind speeds below 3 m/s. This is the case for cloudiness in octants, solar insolation in J/cm^2, and cloudiness in %. The obtained results are logical, because at low wind speed, the influence of this factor (as disturbance) will be the lowest. R^2 for the analyzed external factors, in the case of multi-family residential buildings, is 0.8074 (for *Cloud_2*), 0.9037 (for *S_insol*), and 0.8482 (for *Cloud_1*). In turn, for public buildings, the values of the determination coefficients for the wind speed range below 3 m/s were lower (than for residential buildings) and they were 0.8284 (for *Cloud_2*), 0.8251 (for *S_insol*), and 0.8003 (for *Cloud_1*).

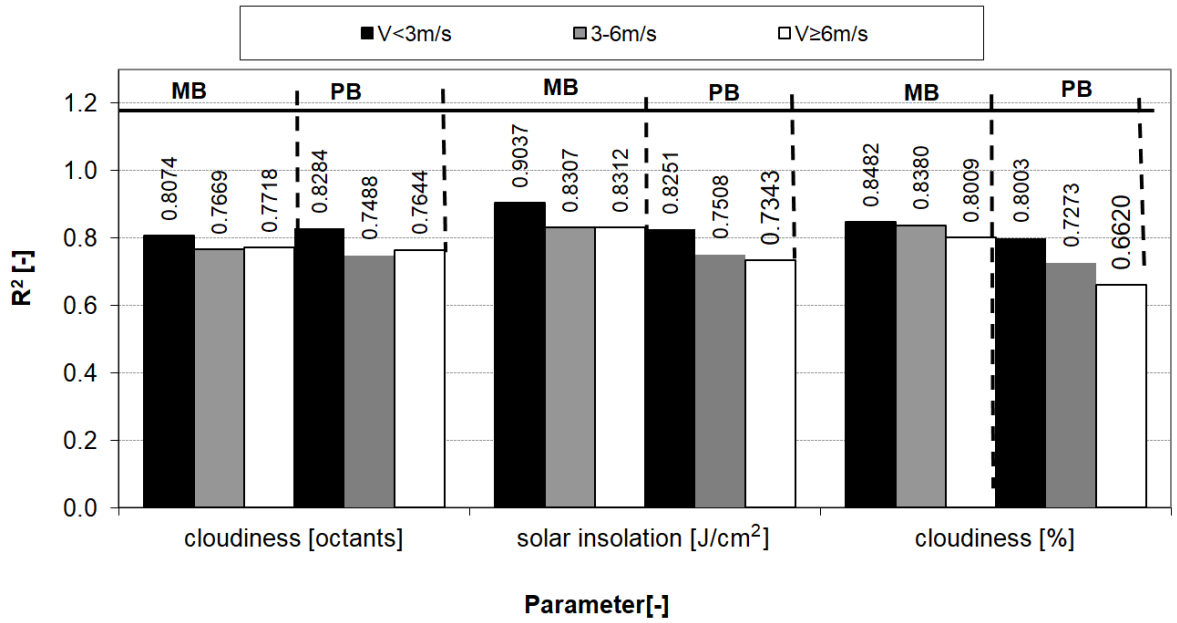

Figure 4. Average determination coefficients for the analyzed external factors related to solar radiation (*S_insol*, *Cloud_1*, and *Cloud_2*), divided into three wind speed ranges for the analyzed multi-family buildings (MB) and public buildings (PB).

On the basis of Figure 4, the mean values of the determination coefficients for cloudiness in octants and cloudiness in percent were also compared. Cloudiness in percent showed visibly higher R^2 values for residential buildings, and this was the case for $v < 3$ m/s, $3 \leq v < 6$ m/s, and $v \geq 6$ m/s. For example, for wind speeds below 3 m/s, R^2 for cloudiness in percent is greater by 5.05% than R^2 for cloudiness in octants.

Then, in order to decide which of the analyzed hourly ranges (6 am–6 pm or 10 am–2 pm) is the most reliable and shows the lowest disturbances (the highest coefficient of determination), the value of arithmetic means of the determination coefficients were also calculated. Figure 5 shows the average coefficients of determination for all the analyzed five multi-family residential buildings and two public buildings, for each of the considered hourly ranges, and for the wind speeds below 3 m/s, without division into their average and maximum values.

From Figure 5, it can be concluded that higher average coefficients of determination occur at 10 am–2 pm. This relationship, although more visible for *Cloud_1*, is also visible for *S_insol* for residential buildings. This is due to the minimization of the influence of system users on heat consumption between 10 am and 2 pm, because residents are not at home due to their work or study, and thus the indoor temperature settings are not changed by, for example, adjusting the position of the thermostatic head by thermostatic radiator valves.

This relationship looks different in the case of average determination coefficients for public buildings. In the case of the results for the cloudiness effect, a much higher R^2 (by 6.2%) for the 10 am–2 pm interval is visible, but in the case of solar insolation, a higher (by 1.5%) average determination coefficient was obtained for the 6 am–6 pm. This may be caused by a much greater influence of the people staying in public buildings (compared to residential buildings) also at 10 am–2 pm, which may disrupt the operation of the heating system by generating internal heat gains and other behaviors.

Another aspect analyzed is whether the use of average or maximum wind speed in a given hour in the analysis is recommended and has an impact on the obtained determination coefficients of characteristic equations for the analyzed factors determining the influence of solar radiation on heat consumption for heating purposes. Figure 6 summarizes the average determination coefficients for cloudiness (%) and solar insolation (J/cm^2), separately for average and maximum wind speeds for the wind speed variant below 3 m/s, and with division into multi-family buildings and public buildings.

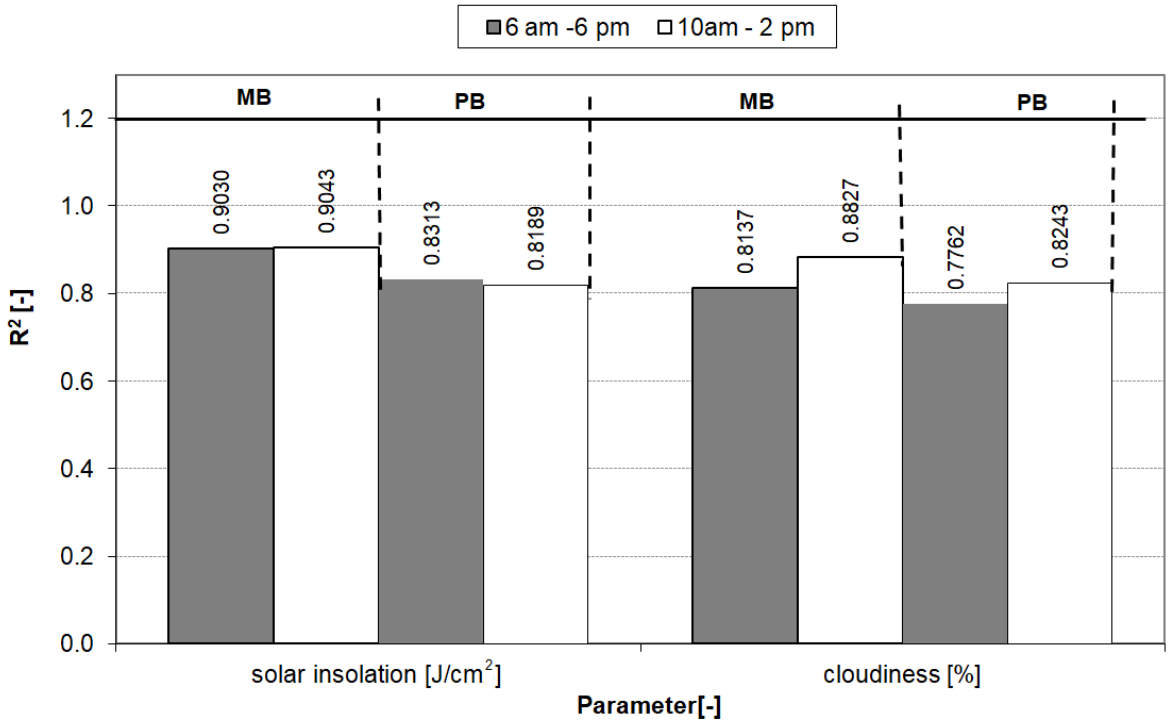

Figure 5. Average values of the determination coefficients for the analyzed external factors, divided into two hourly ranges (6 am–6 pm and 10 am–2 pm) of the input data range for multi-family buildings (MB) and public buildings (PB).

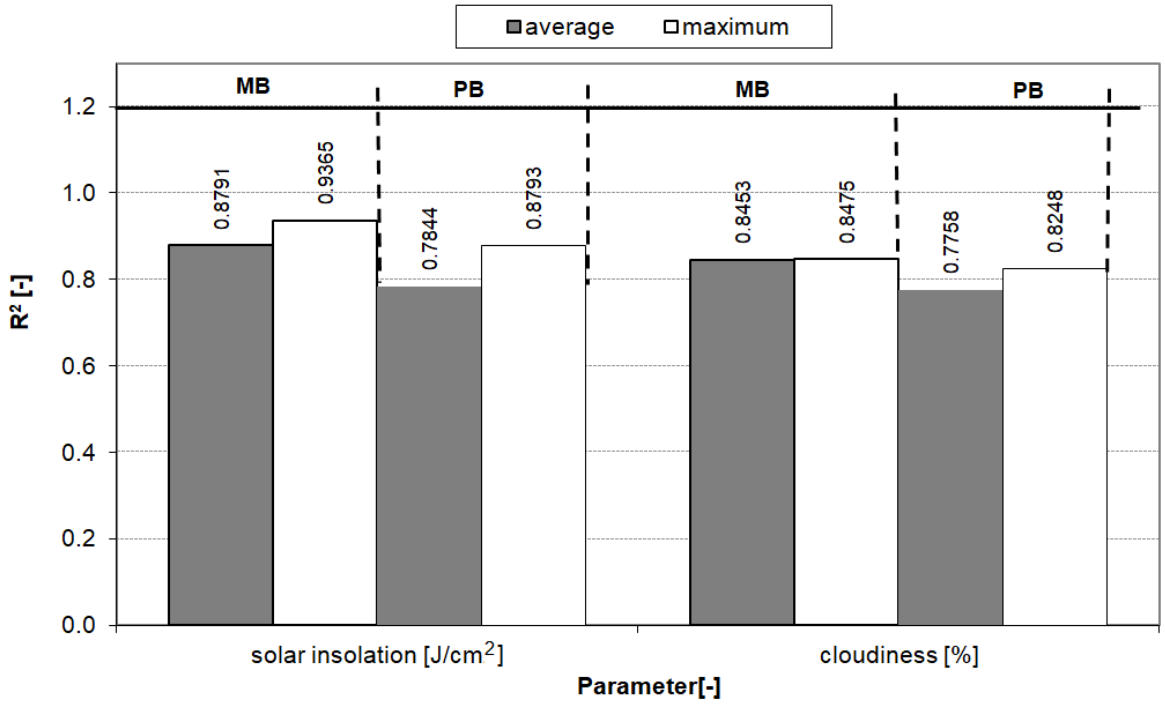

Figure 6. Average determination coefficients for the analyzed external factors, and for average and maximum wind speed below 3 m/s for multi-family buildings (MB) and public buildings (PB).

On the basis of the results presented in Figure 6, it can be concluded that higher determination coefficients are obtained, taking into account the maximum wind speed values in the analyses, rather than the average values. This is the case for both solar insolation and cloudiness for multi-family residential buildings and public buildings. This is due to the fact that taking into account the maximum wind speed minimizes, to a greater

extent, the influence of wind speed as an external factor on disturbances in the process of determining the influence of solar radiation on the heat power supplied to buildings for heating purposes. However, the problem in this case may be that only some weather services have data on the maximum wind speed.

Despite these observations, next stage (in Section 3.2) analyzed both the variants of the average and the maximum wind speed, as they contribute to the high R^2 values, especially in the case of multi-family buildings.

On the basis of the above-mentioned detailed results and their analyses, it was found that it was justified to use, in further considerations, only the data from 10 am to 2 pm for the average and maximum wind speed below 3 m/s, which guarantees the best possible consideration of the influence of both solar insolation and cloudiness on the amount of heat power used for heating. This approach to the issue minimizes the influence of both wind speed and system users as disturbing factors, which usually occur in parallel with solar insolation/cloudiness and may result in incorrect consideration of the influence of the analyzed external factors on the demand and prediction of heat power for heating the buildings.

This will allow, using a universal calculation algorithm, development of appropriate equations correcting the outdoor air temperature, separately for each building, which will appropriately take into account the influence of solar insolation or cloudiness, which was presented in Section 3.2.

3.2. Correction of the Outdoor Temperature Due to Solar Radiation

On the basis of the narrowed range of input data (see Section 3.1), the correction of the outdoor temperature due to solar insolation in J/cm^2 (*S_insol*) and cloudiness in % (*Cloud_1*) was determined separately for each building, because each building may react differently to specific weather conditions. An example of determining the outdoor temperature correction both in terms of wind speed and solar insolation has already been presented by the authors in the article [20].

Nevertheless, for the purposes of this article, an example of determining the outdoor temperature correction due to *S_insol* on the example of a multi-family building, B5, is presented below.

In this process, the correlation equations were used for four sun exposure ranges (0–35 J/cm^2, 35–100 J/cm^2, 100–200 J/cm^2, and >200 J/cm^2) and five cloud cover ranges (0–20%, 20–40%, 40–60%, 60–80%, and 80–100%), which were worked out as part of the calculations in Section 3.1. Using these correlation equations, the values of heat power delivered to buildings were determined for the outdoor temperature range of −20 °C–10 °C (see Table 4).

Then, taking into account the fact that the correlation equations were determined for specific data, the mean insolation was calculated for each of the ranges from which the correlation equations were determined. Lastly, the largest possible logical range was selected (i.e., when an increase in solar insolation leads to a decrease in heat power, and an increase in cloudiness leads to an increase in heat power).

The next step was to determine the increase in the outdoor temperature (N), which was a preliminary correction of the outdoor temperature in the correlation equation for lower solar insolation, enabling us to obtain an identical result of heat power for higher solar insolation. In the case of the example in Table 4, in order to determine the initial correction of the outdoor temperature between the solar insolation ranging from 0–35 J/cm^2 to 35–100 J/cm^2. This calculation was performed according to the following method (Equations (1) and (2)).

$$-3.0363 \cdot (t_e + N) + 51.569 = -2.6536 \cdot t_e + 49.119 \quad (1)$$

$$N = \frac{-2.6536 \cdot t_e + 49.119 - 51.569}{-3.0363} - t_e \quad (2)$$

Using Equation (2), the values presented in column three of Table 5 were calculated. Analogous calculations were performed between successive solar insolation intervals and for all values of the outdoor temperature (from −20 °C to 6 °C).

Table 4. The results of calculations of the heat power (kW) supplied to the multi-family building B5 for heating, for the data range from 10 am to 2 pm, by an average wind speed of v < 3 m/s.

	Solar Insolation (J/cm^2)			
	0–35	**35–100**	**100–200**	**>200**
Outdoor Temperature (°C)	**y = −3.0363x + 51.569**	**y = −2.6536x + 49.119**	**y = −2.572x + 46.783**	**y = −1.8021x + 39.18**
10	21.206	22.583	21.063	21.159
9	24.2423	25.2366	23.635	22.9611
8	27.2786	27.8902	26.207	24.7632
7	30.3149	30.5438	28.779	26.5653
6	33.3512	33.1974	31.351	28.3674
5	36.3875	35.851	33.923	30.1695
4	39.4238	38.5046	36.495	31.9716
3	42.4601	41.1582	39.067	33.7737
2	45.4964	43.8118	41.639	35.5758
1	48.5327	46.4654	44.211	37.3779
0	51.569	49.119	46.783	39.18
−1	54.6053	51.7726	49.355	40.9821
−2	57.6416	54.4262	51.927	42.7842
−3	60.6779	57.0798	54.499	44.5863
−4	63.7142	59.7334	57.071	46.3884
−5	66.7505	62.387	59.643	48.1905
−6	69.7868	65.0406	62.215	49.9926
−7	72.8231	67.6942	64.787	51.7947
−8	75.8594	70.3478	67.359	53.5968
−9	78.8957	73.0014	69.931	55.3989
−10	81.932	75.655	72.503	57.201
−11	84.9683	78.3086	75.075	59.0031
−12	88.0046	80.9622	77.647	60.8052
−13	91.0409	83.6158	80.219	62.6073
−14	94.0772	86.2694	82.791	64.4094
−15	97.1135	88.923	85.363	66.2115
−16	100.1498	91.5766	87.935	68.0136
−17	103.1861	94.2302	90.507	69.8157
−18	106.2224	96.8838	93.079	71.6178
−19	109.2587	99.5374	95.651	73.4199
−20	112.295	102.191	98.223	75.222

In the next step, the sums of preliminary outdoor temperature corrections between successive variants of the increase in the average solar insolation were determined (see Table 6). The value for solar insolation of 0–35 J/cm^2 was now used as a reference value. The process was that for the second average insolation value. The initial temperature corrections from the previous step were copied. For the last two mean solar insolation values, the preliminary temperature corrections presented in Table 5 were summed up. For example, for solar insolation >200 J/cm^2 for −3 °C, it was 6.011675827 (see Table 6), because we added preliminary temperature corrections from the solar insolation ranges 35–100 J/cm^2,

100–200 J/cm^2, and >200 J/cm^2, i.e., 1.18502783, 0.972565571, and 3.854082426, respectively, from Table 6. Then, the average values of the temperature correction for the successive variants of the average solar insolation value (in the range 35–100 J/cm^2 equal to 62.68 J/cm^2, in the range 100–200 J/cm^2 equal to 148.31 J/cm^2, and in the range >200 J/cm^2 equal to 266.52 J/cm^2) were calculated and amounted to 1.689194, 2.784762, and 7.836201.

Table 5. Preliminary correction of the outdoor temperature, example for a multi-family building *B5*.

	Solar Insolation (J/cm^2)			
	0–35	**35–100**	**100–200**	**>200**
Outdoor Temperature (°C)	**y = −3.0363x + 51.569**	**y = −2.6536x + 49.119**	**y = −2.572x + 46.783**	**y = −1.8021x + 39.18**
6		0.050653756	0.695809466	1.160031104
5		0.17669532	0.726560145	1.45937014
4		0.302736884	0.757310823	1.758709176
3		0.428778447	0.788061501	2.058048212
2		0.554820011	0.81881218	2.357387247
1		0.680861575	0.849562858	2.656726283
0		0.806903139	0.880313536	2.956065319
−1		0.932944702	0.911064215	3.255404355
−2		1.058986266	0.941814893	3.55474339
−3		1.18502783	0.972565571	3.854082426
−4		1.311069394	1.00331625	4.153421462
−5		1.437110957	1.034066928	4.452760498
−6		1.563152521	1.064817606	4.752099533
−7		1.689194085	1.095568285	5.051438569
−8		1.815235649	1.126318963	5.350777605
−9		1.941277212	1.157069641	5.650116641
−10		2.067318776	1.18782032	5.949455677
−11		2.19336034	1.218570998	6.248794712
−12		2.319401904	1.249321676	6.548133748
−13		2.445443467	1.280072355	6.847472784
−14		2.571485031	1.310823033	7.14681182
−15		2.697526595	1.341573711	7.446150855
−16		2.823568159	1.37232439	7.745489891
−17		2.949609722	1.403075068	8.044828927
−18		3.075651286	1.433825746	8.344167963
−19		3.20169285	1.464576424	8.643506998
−20		3.327734414	1.495327103	8.942846034

On the basis of the mean values of the outdoor temperature correction determined in this way and the corresponding mean values of solar insolation, Figure 7 was developed, and a correlation equation was determined. This is the correction of the outdoor temperature due to solar insolation for the analyzed multi-family building B5.

Thus, the correction of the outdoor temperature (T_e^{eq}) due to *S_insol* for the example building, B5, can be calculated from Equation (3).

$$T_e^{eq} = t_e + (0.0309 \cdot n - 0.8192), \quad (3)$$

where:

T_e^{eq}—outdoor temperature correction, taking into account solar insolation (in the case of cloudiness, the formula looks similar, there are only other numerical values), °C;

t_e—outdoor air temperature, °C;

n—solar insolation (marked as z in the case of cloudiness), J/cm^2 (in the case of cloudiness, %).

The same was done in the case of *Cloud_1*, and on this basis, corrections of the outdoor temperature due to *S_insol* and *Cloud_1* for the analyzed buildings were determined and are presented in Table 7.

Table 6. Sum of the preliminary outdoor air temperature correction values, example for a multi-family building, B5.

		Mean Solar Insolation (J/cm^2)		
Outdoor Temperature (°C)	**16.24**	**62.68**	**148.31**	**266.52**
6		0.050654	0.746463	1.906494
5		0.176695	0.903255	2.362626
4		0.302737	1.060048	2.818757
3		0.428778	1.21684	3.274888
2		0.554820	1.373632	3.731019
1		0.680862	1.530424	4.187151
0		0.806903	1.687217	4.643282
−1		0.932945	1.844009	5.099413
−2		1.058986	2.000801	5.555545
−3		1.185028	2.157593	6.011676
−4		1.311069	2.314386	6.467807
−5		1.437111	2.471178	6.923938
−6		1.563153	2.62797	7.38007
−7		1.689194	2.784762	7.836201
−8		1.815236	2.941555	8.292332
−9		1.941277	3.098347	8.748463
−10		2.067319	3.255139	9.204595
−11		2.193360	3.411931	9.660726
−12		2.319402	3.568724	10.11686
−13		2.445443	3.725516	10.57299
−14		2.571485	3.882308	11.02912
−15		2.697527	4.0391	11.48525
−16		2.823568	4.195893	11.94138
−17		2.949610	4.352685	12.39751
−18		3.075651	4.509477	12.85364
−19		3.201693	4.666269	13.30978
−20		3.327734	4.823062	13.76591
Average		**1.689194**	**2.784762**	**7.836201**

Table 7. Equations of the equivalent outdoor temperature corrected due to solar insolation or cloudiness.

Building	Parameter	Wind Speed	Equation
B1	solar insolation (J/cm^2)	average	$t_e + (0.0162n + 0.097)$
		maximum	$t_e + (0.0277n - 0.7383)$
	cloudiness (%)	average	$t_e + (-0.0364z + 4.1243)$
		maximum	$t_e + (-0.0533z + 6.1008)$
B2	solar insolation (J/cm^2)	average	$t_e + (0.0311n - 1.411)$
		maximum	$t_e + (0.0133n - 0.1827)$
	cloudiness (%)	average	$t_e + (-0.0489z + 5.2973)$
		maximum	$t_e + (-0.0671z + 6.7361)$
B3	solar insolation (J/cm^2)	average	$t_e + (0.0269n - 1.0419)$
		maximum	$t_e + (0.0102n - 0.1478)$
	cloudiness (%)	average	$t_e + (-0.0891z + 8.5884)$
		maximum	$t_e + (-0.0832z + 6.7708)$
B4	solar insolation (J/cm^2)	average	$t_e + (0.0209n - 0.7183)$
		maximum	$t_e + (0.0377n - 2.2845)$
	cloudiness (%)	average	$t_e + (-0.0169z + 1.8574)$
		maximum	$t_e + (-0.0694z + 5.7688)$
B5	solar insolation (J/cm^2)	average	$t_e + (0.0309n - 0.8192)$
		maximum	$t_e + (0.0205n - 0.1347)$
	cloudiness (%)	average	$t_e + (-0.0257z + 2.4261)$
		maximum	$t_e + (-0.096z + 7.024)$
B6	solar insolation (J/cm^2)	average	$t_e + (0.0302n - 4.5632)$
		maximum	$t_e + (0.007n - 0.0983)$
	cloudiness (%)	average	$t_e + (-0.0055z + 0.4776)$
		maximum	$t_e + (-0.0258z + 1.9022)$
B7	solar insolation (J/cm^2)	average	$t_e + (0.105n - 16.683)$
		maximum	$t_e + (0.0033n - 0.0499)$
	cloudiness (%)	average	$t_e + (-0.1532z + 13.66)$
		maximum	$t_e + (-0.0816z + 8.0567)$

The relationship in the form of the T_e^{eq} allows determination of the influence of external factors, in particular, solar insolation/cloudiness on the heat power supplied to the heating system.

Taking into account the obtained results, it can be concluded that the approach that considers the correction equations developed on the basis of the data for solar insolation and average wind speed is characterized by the highest accuracy and logic of the obtained relationships (see Figure 8). This is due to the larger logical ranges of data observed at this stage for the analyzed variants.

Additionally, it should be noted that cloudiness was determined in octants or percentages, which are not precise parameters (compared to solar insolation), but rather subjective and estimated without the use of precise measuring instruments. These parameters do not take into account the position of the Sun in the sky, which affects the amount of solar radiation reaching and generating heat gains in the analyzed buildings. Therefore, as a more reliable parameter (the average value of the determination coefficient for the equations of

the outdoor temperature correction due to solar radiation for the analyzed buildings at the level of 0.885), it is recommended to use solar insolation to take into account the influence of solar radiation on the heat power supplied to the building for heating.

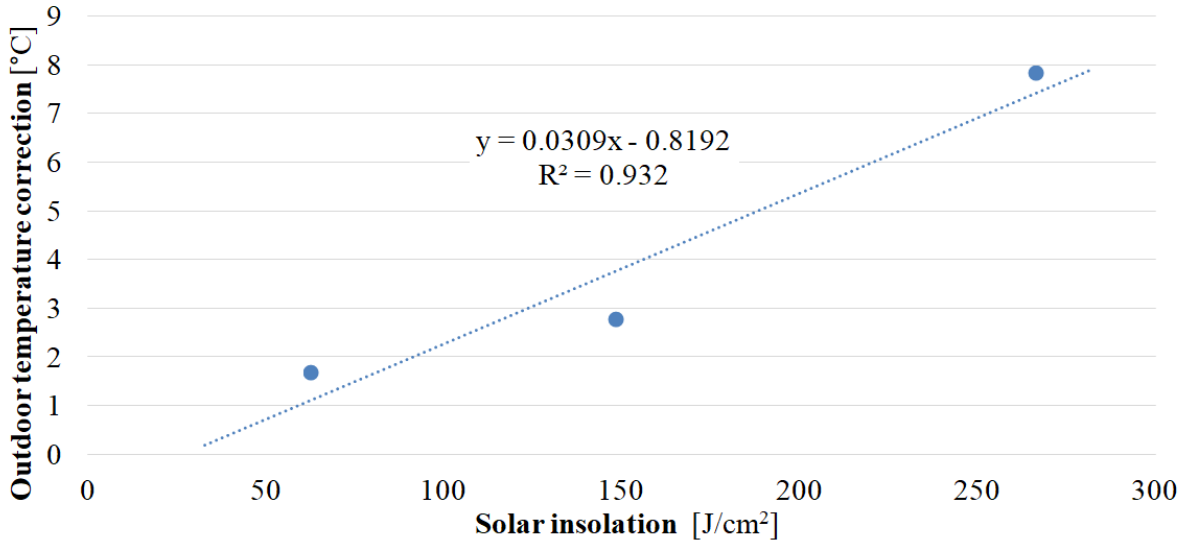

Figure 7. Outdoor temperature correction (°C) depending on the solar insolation (J/cm^2).

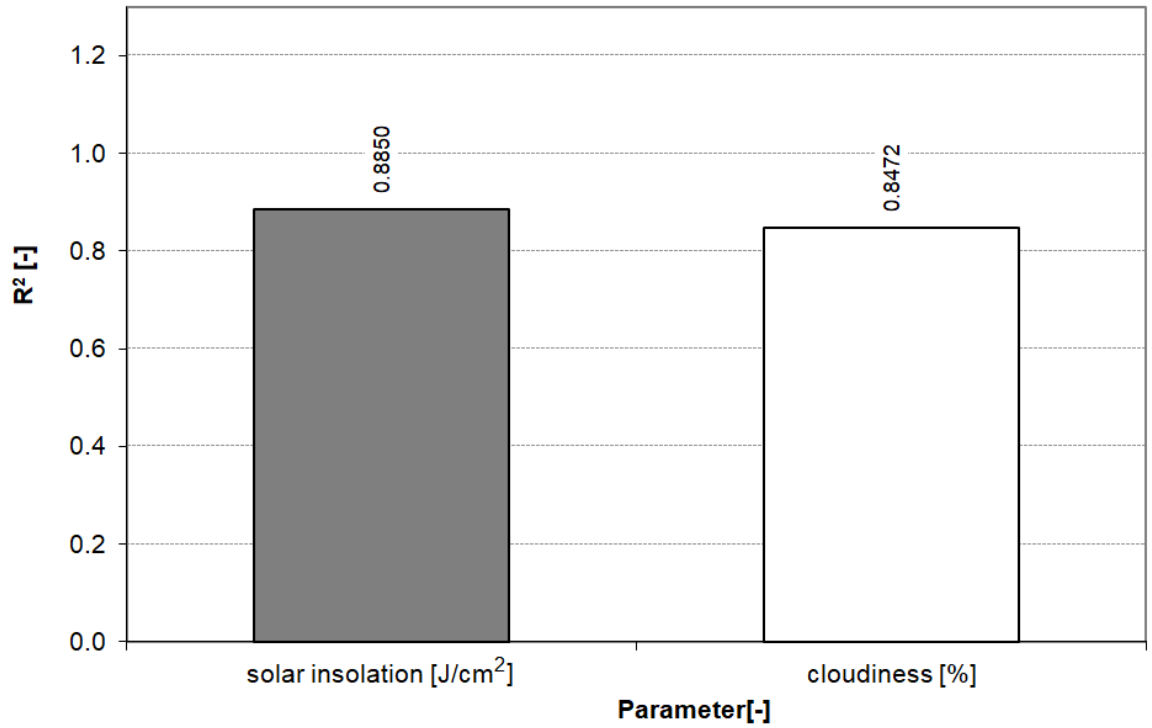

Figure 8. Average determination coefficients of the equations of the outdoor temperature correction for solar insolation/cloudiness by average wind speed.

4. Conclusions

This work proposed a universal calculation algorithm that will allow determination of the actual impact of solar radiation on the heat power supplied to a room or building for heating purposes, and thus it will be able to counteract the phenomenon of overheating rooms and reduce heat consumption.

Each analyzed building reacted differently to external factors related to solar radiation (in particular, cloudiness or solar insolation), which results from the individual structure of the building, its orientation, ventilation system, tightness, and behavior of occupants.

Therefore, in the first place, a detailed and multi-variant analysis of the impact of external factors related to solar radiation (*S_insol*, *Cloud_1*, and *Cloud_2*) on the heat power supplied to the building for heating purposes was carried out with different ranges of hourly data included in the analysis and wind speed values, to appropriately narrow down the range of input data included in the calculations.

On the basis of the conducted research, it was found that it was justified to narrow down the scope of data included in the calculations (narrowing down to 10 am–2 pm, at wind speeds below 3 m/s) in order to minimize the disturbances caused particularly by wind and building users. This was due to the fact that for such a narrowed range of data, the correlation equations for solar insolation or cloudiness from the outdoor temperature were obtained, which were characterized by high average values of determination coefficients at the level of 0.9043 (for solar insolation) and 0.8827 (for cloudiness in %) for the analyzed residential buildings.

Additionally, when determining the outdoor temperature correction due to the influence of solar radiation, it was found that the obtained results for solar insolation were more accurate (R^2 = 0.8850) than for cloudiness (R^2 = 0.8472). Therefore, it was recommended to use solar insolation as a parameter as it was more reliable than cloudiness in the calculations of a building energy model.

Besides, it was noticed that because of the simplicity of the method, it was not required to know the emissivity of the building or its parts, solar absorptivity, or surface temperatures of parts of the building (windows, walls, and roof), which necessitates conducting additional measurements and very detailed calculations.

This was connected with the fact that this simple method was based on real data, which were analyzed in a specific way (described above) in order to extract the influence of solar heat gain in the form of solar radiation on thermal power for heating of buildings.

Further research in this area may be focused on the development of methods of controlling heating systems, which, taking into account external factors (in particular, solar insolation) and the factors related to the behavior and preferences of users of heating systems, will allow forecast of the heat power demand and optimize its supply to achieve high energy savings while maintaining the thermal comfort of users.

Author Contributions: Study conception and design: T.C.; Acquisition, analysis, and interpretation of data: T.C., A.M., and A.S.-O.; Drafting of manuscript: T.C., A.M., A.S.-O., A.S., P.M., P.W., Ł.G., M.R.D., and K.Ł.; Critical revision: T.C., A.M., A.S.-O., A.S., P.M., P.W., Ł.G., M.R.D., and K.Ł. All authors have read and agreed to the published version of the manuscript.

Funding: This study was supported by research project, financed from European Funds (under the Intelligent Development Programme) by the Polish National Centre for Research and Development. Project number: POIR.04.01.02-00-0012/18.

Institutional Review Board Statement: Not applicable.

Informed Consent Statement: Not applicable.

Data Availability Statement: The data presented in this study are available on request from the corresponding author.

Acknowledgments: Authors would like to thank Rafał Michałowski (a student of the Lublin University of Technology) for participating in the research. Unfortunately, he passed away before we started to write this article.

Conflicts of Interest: The authors declare no conflict of interest. The funders had no role in the design of the study; in the collection, analyses, or interpretation of data; in the writing of the manuscript; or in the decision to publish the results.

References

1. Frattolillo, A.; Canale, L.; Ficco, G.; Mastino, C.C.; Dell'Isola, M. Potential for Building Façade-Integrated Solar Thermal Collectors in a Highly Urbanized Context. *Energies* **2020**, *13*, 5801. [CrossRef]
2. Bianco, L.; Komerska, A.; Cascone, Y.; Serra, V.; Zinzi, M.; Carnielo, E.; Ksionek, D. Thermal and optical characterisation of dynamic shading systems with PCMs through laboratory experimental measurements. *Energy Build.* **2018**, *163*, 92–110. [CrossRef]
3. Baccoli, R.; Frattolillo, A.; Mastino, C.; Curreli, S.; Ghiani, E. A comprehensive optimization model for flat solar collector coupled with a flat booster bottom reflector based on an exact finite length simulation model. *Energy Convers. Manag.* **2018**, *164*, 482–507. [CrossRef]
4. Ménard, R.; Souviron, J. Passive solar heating through glazing: The limits and potential for climate change mitigation in the European building stock. *Energy Build.* **2020**, *228*, 110400. [CrossRef]
5. Kumar, K.; Saboor, S.; Kumar, V.; Kim, K.H.; Babu, T.P.A. Experimental and theoretical studies of various solar control window glasses for the reduction of cooling and heating loads in buildings across different climatic regions. *Energy Build.* **2018**, *173*, 326–336.
6. Porritt, S.M.; Cropper, P.C.; Shao, L.; Goodier, C.I. Ranking of interventions to reduce dwelling overheating during heat waves. *Energy Build.* **2012**, *55*, 16–27. [CrossRef]
7. Fletcher, M.J.; Johnston, D.K.; Glew, D.W.; Parker, J.M. An empirical evaluation of temporal overheating in an assisted living Passivhaus dwelling in the UK. *Build. Environ.* **2017**, *121*, 106–118. [CrossRef]
8. Gamero-Salinas, J.C.; Monge-Barrio, A.; Saanchez-Ostiz, A. Overheating risk assessment of different dwellings during the hottest season of a warm tropical climate. *Build. Environ.* **2020**, *171*, 106664. [CrossRef]
9. Brideau, S.; Beausoleil-Morrison, I.; Kummert, M. Collection and storage of solar gains incident on the floor in a house during the heating season. *Energy Procedia* **2015**, *78*, 2274–2279. [CrossRef]
10. Stamp, S.; Altamirano-Medina, H.; Lowe, R. Measuring and accounting for solar gains in steady state whole building heat loss measurements. *Energy Build.* **2017**, *153*, 168–178. [CrossRef]
11. Danov, S.; Carbonell, J.; Cipriano, J.; Marti-Herrero, J. Approaches to evaluate building energy performance from daily consumption data considering dynamic and solar gain effects. *Energy Build.* **2013**, *57*, 110–118. [CrossRef]
12. Knudsen, M.D.; Petersen, S. Economic model predictive control of space heating and dynamic solar shading. *Energy Build.* **2020**, *209*, 109661. [CrossRef]
13. Afram, A.; Janabi-Sharifi, F. Theory and applications of HVAC control systems—A review of model predictive control (MPC). *Build. Environ.* **2014**, *72*, 343–355. [CrossRef]
14. Wang, Z.; Hong, T. Reinforcement learning for building controls: The opportunities and challenges. *Appl. Energy* **2020**, *269*, 115036. [CrossRef]
15. Bilous, I.; Deshko, V.; Sukhodub, I. Parametric analysis of external and internal factors influence on building energy performance using non-linear multivariate regression models. *J. Build. Eng.* **2018**, *20*, 327–336. [CrossRef]
16. Hong, T.; Wang, Z.; Luo, X.; Zhang, W. State-of-the-art on research and applications of machine learning in the building life cycle. *Energy Build.* **2020**, *212*, 109831. [CrossRef]
17. Wang, R.; Lu, S.; Feng, W. A novel improved model for building energy consumption prediction based on model integration. *Appl. Energy* **2020**, *262*, 114561. [CrossRef]
18. D'Amico, A.; Ciulla, G.; Tupenaite, L.; Kaklauskas, A. Multiple criteria assessment of methods for forecasting building thermal energy demand. *Energy Build.* **2020**, *224*, 110220. [CrossRef]
19. Turski, M.; Sekret, R. Buildings and a District Heating Network as Thermal Energy Storages in the District Heating System. *Energy Build.* **2018**, *179*, 49–56. [CrossRef]
20. Cholewa, T.; Siuta-Olcha, A.; Smolarz, A.; Muryjas, P.; Wolszczak, P.; Anasiewicz, R.; Balaras, C.A. A simple building energy model in form of an equivalent outdoor temperature. *Energy Build.* **2021**, in press. [CrossRef]